

- that an increase of the activation energy becomes plausible.
27. H. Conrad, G. Ertl, J. Küppers, *Surf. Sci.* **76**, 323 (1978).
28. M. A. Barteau, E. I. Ko, R. J. Madix, *ibid.* **104**, 161 (1981).

29. J. A. Dumesic, D. F. Rudd, L. M. Aparicia, J. E. Rekoske, A. A. Trivino, *The Microkinetics of Heterogeneous Catalysis* (American Chemical Society, Washington, DC, 1993).

18 August 1997; accepted 30 October 1997

Growth of SiO₂ at Room Temperature with the Use of Catalyzed Sequential Half-Reactions

Jason W. Klaus, Ofer Sneh,* Steven M. George†

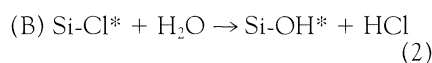
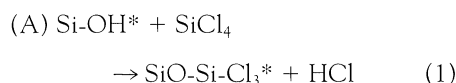
Films of silicon dioxide (SiO₂) were deposited at room temperature by means of catalyzed binary reaction sequence chemistry. The binary reaction SiCl₄ + 2H₂O → SiO₂ + 4HCl was separated into SiCl₄ and H₂O half-reactions, and the half-reactions were then performed in an ABAB . . . sequence and catalyzed with pyridine. The pyridine catalyst lowered the deposition temperature from >600 to 300 kelvin and reduced the reactant flux required for complete reactions from ~10⁹ to ~10⁴ Langmuirs. Growth rates of ~2.1 angstroms per AB reaction cycle were obtained at room temperature for reactant pressures of 15 millitorr and 60-second exposure times with 200 millitorr of pyridine. This catalytic technique may be general and should facilitate the chemical vapor deposition of other oxide and nitride materials.

The reduction of thin films to nanometer dimensions for new technologies requires exquisite control of film thickness, morphology, crystallinity, and conformality (1). Lower deposition temperatures are also required because interlayer diffusion may destroy the properties of nanoscale devices. Many of these requirements can be achieved by growth controlled at single atomic layers by means of binary reaction sequence chemistry (2).

SiO₂ is the optimal dielectric material in silicon microelectronic devices. Conformal SiO₂ film deposition on trench capacitors with high aspect ratios will be needed as interface layers to extend dynamic random access memory (DRAM) to the 1-gigabyte regime (3). Future flat panel displays will require uniform and precise SiO₂ film deposition on extremely large substrates (4). In addition, very thin SiO₂ films can be used in multilayer and nanolaminate structures to tailor mechanical, electrical, and optical thin film properties (5). Low-temperature SiO₂ deposition techniques will also facilitate the use of SiO₂ as a protective coating or insulator on polymeric or biological materials.

Self-terminating surface reactions applied in a binary reaction sequence can be used to achieve atomic layer control of thin film growth (2, 6–9). Recent work on SiO₂ atomic layer-controlled growth has focused

on dividing the SiCl₄ + 2H₂O → SiO₂ + 4HCl reaction into two half-reactions (6):



where the asterisks designate the surface species. The SiCl₄ and H₂O half-reactions are performed in an ABAB . . . binary sequence to grow SiO₂.

In each half-reaction, a gas-phase precursor reacts with a surface functional group. The surface reaction continues until all of the initial surface functional groups have reacted and have been replaced with the new functional group. Successive application of the A and B half-reactions has produced atomic layer-controlled SiO₂ deposition (9). Atomic force microscope (AFM) images revealed that the SiO₂ films deposited on Si(100) were highly conformal and extremely smooth (9). The only drawback was the high temperatures (>600 K) and large reactant exposures [$>10^9$ Langmuirs (1 L = 10⁻⁶ torr s)] required for the surface half-reactions to reach completion.

We now show that high reaction temperatures and large precursor fluxes can be avoided by catalyzing the surface reactions. We chose the organic base pyridine (C₅H₅N) as the catalyst because pyridine interacts strongly with the surface functional groups and reactants present during both the SiCl₄ and H₂O half-reactions of the binary reaction sequence (10). Pyridine is also a very stable molecule, and this stability minimized incorporation of N or C into

the deposited SiO₂ film.

We observed no uncatalyzed SiO₂ film growth on our Si(100) wafer at 300 K after five AB cycles for reactant exposures as large as 10¹⁰ L during the A and B half-reactions (11). In contrast, the addition of a small amount of pyridine initiated immediate SiO₂ film growth. The effect of pyridine was quantified by measuring SiO₂ film deposition as a function of pyridine partial pressure using fixed reactant exposures of 15 mtorr for 15 s. Pyridine accelerated the half-reactions with increasing pyridine partial pressures up to 2.0 torr. Pressures greater than 2.0 torr resulted in no further measurable enhancement of the reaction efficiency.

The dependence of the half-reactions on the A and B reactant exposure time (reactant pressure, 15 mtorr) was examined by measuring the SiO₂ film thickness deposited by five AB cycles at 290 K (Fig. 1). The pyridine partial pressure was fixed at 200 mtorr to allow shorter pumping times between the reaction cycles. The SiCl₄ exposure times were equal to the H₂O exposure times. A typical AB cycle occurred with the following sequence: Expose pyridine (200 mtorr); dose SiCl₄ (15 mtorr) for variable reaction times; evacuate (10⁻⁴ torr); expose pyridine (200 mtorr); dose H₂O (15 mtorr) for variable reaction times; evacuate (10⁻⁴ torr).

The half-reactions are self-limiting; once a half-reaction goes to completion, additional reactant produces no additional film growth. To determine which half-reaction is slower, we studied the SiO₂ film growth versus H₂O exposure time with a fixed SiCl₄ exposure time. The SiCl₄ and H₂O pressures were equal. The SiO₂ growth rate did not decrease until the H₂O exposure time was one-fourth that of the SiCl₄ exposure time, which indicates that the SiCl₄

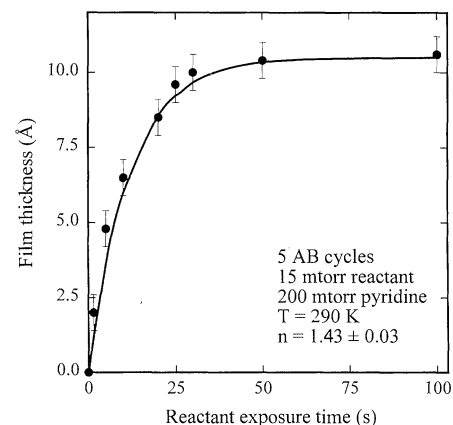


Fig. 1. Ellipsometric measurements of SiO₂ film thickness deposited by five AB cycles at 290 K for various reactant exposure times at reactant pressures of 15 mtorr with 200 mtorr of pyridine.

Department of Chemistry and Biochemistry, University of Colorado, Boulder, CO 80309, USA.

*Present address: Lucent Technologies—Bell Laboratories, Optoelectronics Center, Breinigsville, PA 18031, USA.

†To whom correspondence should be addressed.

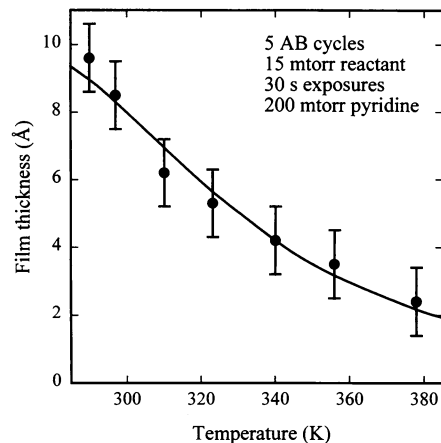


Fig. 2. Ellipsometric measurements of SiO₂ film thickness deposited by five AB cycles for various substrate temperatures at reactant pressures of 15 mtorr for 30 s with 200 mtorr of pyridine.

half-reaction is about one-fourth as fast as the H₂O half-reaction. In addition, the SiO₂ growth at the shortest SiCl₄ exposure time, 5 s, did not increase with H₂O exposure for exposure times as long as 60 s. This observation implies that the SiO₂ film growth in Fig. 1 is controlled by the SiCl₄ half-reaction. Equal reactant exposures were used in all further experiments.

We next fixed the reactant exposures (15 mtorr for 30 s) and catalyst pressure (200 mtorr) and varied the temperature. These conditions were nearly sufficient for complete reaction only at 295 K. The SiO₂ film thickness deposited by five AB cycles decreased with increasing temperature (Fig. 2). The decrease in the deposition rate cannot be attributed to the loss of reactive hydroxyl groups at higher temperatures (2SiOH* → Si-O-Si + H₂O). The hydroxyl coverage decreases only very slightly be-

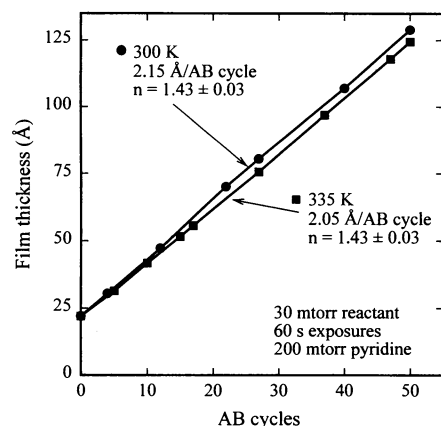


Fig. 3. Ellipsometric measurements of total SiO₂ film thickness deposited on Si(100) at 300 K and 335 K versus number of AB reaction cycles at reactant pressures of 30 mtorr for 60 s with 200 mtorr of pyridine.

tween 300 and 370 K (12). The reduction in growth rate results primarily from the reduction in the surface coverages of reactant and pyridine at the higher temperatures (see below).

The total SiO₂ film thickness on the Si(100) wafer versus the number of AB cycles (30 mtorr for 60 s, 200 mtorr of pyridine) is shown in Fig. 3. These conditions were sufficient for complete reaction. The growth of the SiO₂ film thickness was extremely linear relative to the number of AB cycles. The measured growth rate was 2.15 Å per AB cycle at 300 K and 2.05 Å per AB cycle at 335 K. The constant growth rate implies that the deposited SiO₂ films are not roughening as the number of AB cycles increases. Strong amine bases may form salts that could poison the surface and degrade the reaction efficiency (10). The linear growth rate in Fig. 3 argues against salt formation. The small decrease of the SiO₂ growth rate between 300 K and 335 K can be attributed to a slightly lower hydroxyl coverage at higher substrate temperatures (12).

The surface morphology of the SiO₂ films was studied with an AFM (Digital Instruments Nanoscope III) in tapping mode. Figure 4 shows a 1.2 μm by 1.2 μm scan for a SiO₂ film deposited by 50 AB cycles at 300 K (30 mtorr for 60 s, 200 mtorr of pyridine). The micrographs of the deposited SiO₂ films indicate a surface roughness of ±3 Å (root mean square). In comparison, the surface roughness of the initial cleaned Si(100) wafer was ±2 Å. A SiO₂ film deposited at 700 K without the pyridine catalyst displayed a roughness of ±3 Å. In addition, the power spectrum of the surface roughness of the SiO₂ films deposited at 300 K exhibited the same statistical characteristics as the initial Si(100) wafer and the SiO₂ film grown at 700 K (7). This behavior indicates that the SiO₂ film grows conformally over the Si(100) substrate with negligible roughening.

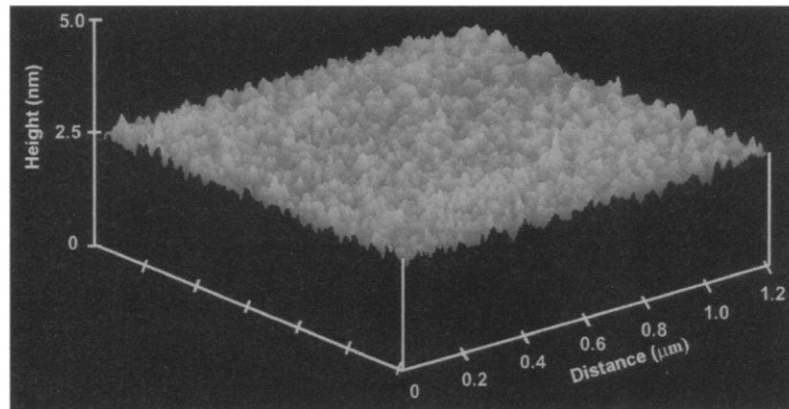


Fig. 4. AFM image of an SiO₂ film deposited at 300 K by 50 AB cycles at reactant pressures of 30 mtorr for 60 s with 200 mtorr of pyridine. The light-to-dark range is 10 Å.

The SiO₂ film quality was evaluated with Rutherford backscattering (RBS) and dielectric breakdown measurements. The RBS measurements showed that the film stoichiometry was 2/1 for O/Si with a precision of ±10% determined by the small (~150 Å) SiO₂ film thickness. The C/Si and N/Si atomic ratios were below the detection threshold of the RBS measurements (<1 to 2%). These small upper limits indicate that the pyridine catalyst is not incorporated into the SiO₂ film. The RBS analysis also revealed that the Cl/Si atomic ratio was <0.2 to 0.5%. This low ratio is consistent with surface reactions that proceed to near completion. In addition, preliminary current-voltage measurements displayed dielectric breakdown thresholds similar to those of thermally grown SiO₂ films (13).

Catalysis of the SiO₂ growth lowers the reaction temperatures from >600 K to 300 K and reduces the saturation reactant exposures from ~10⁹ L to ~10⁴ L. The proposed mechanism of the catalytic activation suggested earlier by vibrational studies (10) is shown in Fig. 5. The Si-OH* surface species are known to have strong interactions with Lewis bases such as pyridine. The adsorption energy of pyridine on hydroxylated high-surface area silica ranges from 15 to 17 kcal mol⁻¹ (14). The hydrogen-bonding portion of this interaction substantially weakens the Si-O-H bond and increases the nucleophilicity of the O atom for attack on the electron-deficient Si during the SiCl₄ half-reaction (10).

The H₂O half-reaction is also catalyzed by the pyridine. The addition of pyridine could accelerate the reaction by hydrogen-bonding with the H₂O reactant and thus making the O atom more nucleophilic. This increased nucleophilicity would facilitate the attack of the O atom on the electron-deficient surface Si atoms. Another possible catalytic pathway is the direct interaction of the N lone pair electrons on pyridine

with the electron-deficient surface Si atoms. This interaction could weaken the Si-Cl bond and facilitate the replacement of the Cl groups with OH groups.

On the basis of the surface reaction mechanism in Fig. 5, a rate equation can be proposed for the SiO₂ growth during the slower SiCl₄ half-reaction,

$$d\Theta/dt = k\Theta_{\text{SiCl}_4}\Theta_{\text{PYR}}(1 - \Theta^*) \quad (3)$$

where k is the reaction rate constant [$k = \nu_0 \exp(-E_r/RT)$, where ν_0 is the preexponential factor, E_r is the activation energy, and R is the gas constant], Θ^* is the coverage of reacted sites, and Θ_{SiCl_4} and Θ_{PYR} are the coverages of the reactant and catalyst, respectively. The $(1 - \Theta^*)$ term is used because the SiCl₄ half-reaction requires a hydroxyl group to interact with pyridine and react with SiCl₄. The above rate equation yields the coverage of reacted sites, Θ^* , as

$$\Theta^* = 1 - \exp[-k\Theta_{\text{SiCl}_4}\Theta_{\text{PYR}}t] \quad (4)$$

This expression was fit to the data in Figs. 1 and 2; Θ_{SiCl_4} was determined by using a SiCl₄ adsorption energy of 5.4 kcal mol⁻¹ (15) on hydroxyl groups on silica surfaces. The pyridine coverage, Θ_{PYR} , was derived using a pyridine adsorption energy of 12.3 kcal mol⁻¹ and a pyridine desorption preexponential of $4.4 \times 10^{14} \text{ s}^{-1}$ on the hydroxylated SiO₂ surface. These parameters were measured with an in situ ellipsometer (16).

The fit to the temperature-dependent data (solid line in Fig. 2) used these SiCl₄ and pyridine adsorption and desorption parameters and assumed a preexponential of 10^{13} s^{-1} for SiCl₄ desorption. This fit yielded a reaction preexponential of $\nu_0 = 3.1 \times 10^{13 \pm 1.1} \text{ s}^{-1}$ and a reaction activation barrier of $E_r = 11.4 \pm 1.1 \text{ kcal mol}^{-1}$.

From 295 to 378 K, Θ_{SiCl_4} at 15 mtorr of SiCl₄ varied from 4.5×10^{-6} monolayers (ML) to 6.0×10^{-7} ML, and Θ_{PYR} at 200 mtorr of pyridine ranged from 0.19 ML to 2.4×10^{-3} ML.

As expected for catalytic behavior, the reaction activation barrier of $E_r = 11.4 \pm 1.1 \text{ kcal mol}^{-1}$ obtained from the fit shown in Fig. 2 is much less than the barrier for the uncatalyzed reaction of SiCl₄ with Si-OH* surface species; E_r without the catalyst has been measured to be 22 kcal mol⁻¹ (17). Equation 4 also gives an excellent fit to the reactant exposure time data in Fig. 1; for the ν_0 and E_r parameters derived from the fit in Fig. 2, Eq. 4 yields the solid line in Fig. 1.

A model for the SiO₂ film growth was also developed under the assumption that the maximum number of Si atoms that can be added during the SiCl₄ half-reaction is equal to the coverage of SiOH* hydroxyl groups (6, 9). The room-temperature hydroxyl coverage has been measured to be $4.6 \pm 0.4 \times 10^{14} \text{ cm}^{-2}$ (12). The coverage of Si atoms and SiO₂ units that is consistent with one monolayer can be derived from the refractive index for SiO₂ of $n = 1.46$. From the Lorenz-Lorentz relation, $n = 1.46$ yields a density of 2.21 g cm^{-3} or a number density of $\rho = 2.2 \times 10^{22} \text{ SiO}_2 \text{ units cm}^{-3}$. The coverage of a SiO₂ monolayer can then be calculated as $\rho^{2/3} = 7.9 \times 10^{14} \text{ SiO}_2 \text{ units cm}^{-2}$. Likewise, $\rho^{-1/3}$ represents a thickness of 3.5 Å for a SiO₂ monolayer. On the basis of the coverage and thickness of a SiO₂ monolayer, the SiO₂ deposition rate predicted by the model is $\sim 2.0 \text{ Å per AB cycle}$. This prediction compares favorably with the measured growth rate of $\sim 2.1 \text{ Å per AB cycle}$.

The catalysis of surface reactions with a gas-phase reagent represents a new paradigm for the improvement of reaction efficiencies in chemical vapor deposition (CVD). CVD reactions are almost never facilitated by catalysts. Catalysis on surfaces is usually viewed only in terms of heterogeneous catalysis where the catalyst is a metal or oxide surface. In contrast, the catalyst in our work is a gas-phase species that enhances the reactivity of the surface species. The applicability of gas-phase catalysts may be general and may be used to grow other technologically important oxide and nitride materials at reduced temperatures.

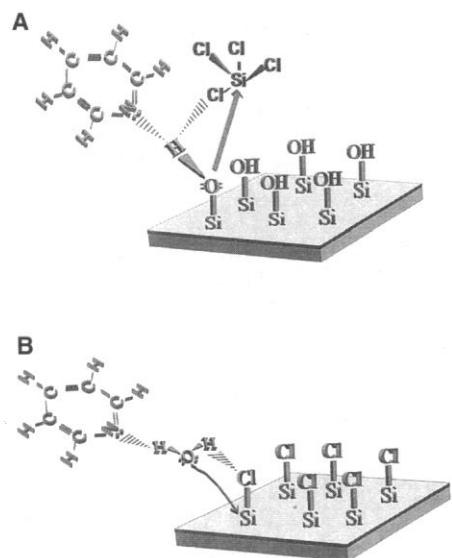


Fig. 5. Proposed mechanism of pyridine catalysis during (A) the SiCl₄ half-reaction and (B) the H₂O half-reaction.

REFERENCES AND NOTES

1. T. Ohmi, *Jpn. J. Appl. Phys.* **33**, 6747 (1994); National Technology Roadmap for Semiconductors, SIA Semiconductor Industry Association, 4300 Stevens Creek Boulevard, San Jose, CA 95129, USA (<http://www.semtech.org/public/roadmap/doc/toc.html>), 1994.
2. S. M. George, A. W. Ott, J. W. Klaus, *J. Phys. Chem.* **100**, 13121 (1996); C. H. L. Goodman and M. V. Pessa, *J. Appl. Phys.* **60**, R65 (1986); T. Suntola, *Thin Solid Films* **216**, 84 (1992).
3. Y. Nakagome and K. Itoh, *IEICE Trans.* **E-74**, 799 (1991).
4. W. C. O'Mara, *Liquid Crystal Flat Panel Displays: Manufacturing Science and Technology* (Van Nostrand Reinhold, New York, 1993).
5. M. Leskela, K. Kukli, J. Ihanus, M. Ritala, *Appl. Phys. Lett.* **68**, 3737 (1996).
6. O. Sneh, M. L. Wise, A. W. Ott, L. A. Okada, S. M. George, *Surf. Sci.* **334**, 135 (1995).
7. A. W. Ott, J. W. Klaus, J. M. Johnson, S. M. George, *Thin Solid Films* **292**, 135 (1996).
8. S. M. George et al., *Appl. Surf. Sci.* **82-83**, 460 (1994).
9. J. W. Klaus, A. W. Ott, J. M. Johnson, S. M. George, *Appl. Phys. Lett.* **70**, 1092 (1997).
10. C. P. Tripp and M. L. Hair, *J. Phys. Chem.* **97**, 5693 (1993).
11. Our experiments were performed in a deposition apparatus that has been described in detail elsewhere (7). In brief, the apparatus consists of a sample load lock chamber, a central deposition chamber (base pressure of 1×10^{-7} torr), and a high-vacuum chamber for surface analysis. The central deposition chamber allows automated dosing of molecular precursors under a wide variety of conditions and is equipped with an in situ spectroscopic ellipsometer (J. A. Woolam Co. M-44). This ellipsometer allows the film thickness and refractive index to be measured accurately during film deposition. In addition, ex situ atomic force microscopy was used to image the surface topography of the SiO₂ films. The substrates, Si(100) wafers, were rinsed with methanol and blown free of particles before loading into the deposition chamber. The Si(100) substrate was annealed at 800 K for 1 min and then exposed to a H₂O plasma at room temperature to remove surface carbon and hydroxylate the surface. This cleaning procedure leaves a SiO₂ native oxide with a thickness of $\sim 20 \text{ Å}$ on the Si(100) surface.
12. O. Sneh and S. M. George, *J. Phys. Chem.* **99**, 4639 (1994).
13. To test the dielectric strength of the SiO₂ films under high field stress conditions, we deposited multiple Au-Ti squares ($125 \mu\text{m}$ by $125 \mu\text{m}$) on the SiO₂ surface. A constant dc voltage was then applied for 5 min to the capacitor electrodes defined by the bottom of the Si substrate and the individual Au-Ti squares. The current was measured with a picoammeter versus stress voltage. A capacitor failure was characterized by a large decrease in film resistance or by a resistance that steadily decreased during the 5-min period. Some capacitors broke down at low-stress fields of $<10 \text{ kV cm}^{-1}$. However, some capacitors did not display an abrupt resistance change even at high-stress fields of $>20 \text{ MV cm}^{-1}$. The majority of the capacitor breakdowns occurred at stress voltages in the range of 4 to 10 MV cm⁻¹. This behavior is similar to the properties of thermally grown oxide films on silicon. Because the substrates were not prepared under cleanroom conditions, the low breakdown voltages measured on some of the capacitors are probably associated with particulate and surface contamination on the substrate.
14. H. Noller and B. Mayerbock, *Surf. Sci.* **33**, 82 (1972); G. Curthoys, V. Y. Davydov, A. V. Kiselev, S. A. Kiselev, B. V. Kuznetsov, *J. Colloid Interface Sci.* **48**, 58 (1974).
15. C. P. Tripp and M. L. Hair, *Langmuir* **8**, 1961 (1992).
16. In these ellipsometric experiments, the pyridine thickness was measured versus pyridine pressure. A fit based on the Brunauer-Emmett-Teller (BET) adsorption model yielded a surface adsorption energy of $12.3 \pm 0.9 \text{ kcal mol}^{-1}$ and a desorption preexponential of $4.4 \times 10^{14 \pm 0.7} \text{ s}^{-1}$.
17. M. L. Hair and W. Hertl, *J. Phys. Chem.* **73**, 2372 (1969).
18. Supported by the U.S. Office of Naval Research and the Air Force Office of Scientific Research.

19 May 1997; accepted 31 October 1997